HHS Public Access

Author manuscript

Gene Ther. Author manuscript; available in PMC 2016 May 19.

Published in final edited form as:

Gene Ther. 2016 February ; 23(2): 135–143. doi:10.1038/gt.2015.105.

Neuroblastomas Vary Widely in Their Sensitivities to Herpes Simplex Virotherapy Unrelated to Virus Receptors and Susceptibility

Pin-Yi Wang[1], **Hayley M. Swain**[1], **Anne L. Kunkler**[1], **Chun-Yu Chen**[1], **Brian J. Hutzen**[1], **Michael A. Arnold**[2], **Keri A. Streby**[3], **Margaret H. Collins**[4], **Betsy Dipasquale**[4], **Joseph R. Stanek**[3], **Joe Conner**[5], **Toin H. van Kuppevelt**[6], **Joseph C. Glorioso**[7], **Paola Grandi**[7], and **Timothy P. Cripe**[1,3]

[1]Center for Childhood Cancer and Blood Diseases, Nationwide Children's Hospital, The Ohio State University, Columbus, OH, USA [2]Department of Pathology, The Ohio State University, Columbus, OH, USA [3]Division of Hematology/Oncology/Blood and Marrow Transplant, Nationwide Children's Hospital, The Ohio State University, Columbus, OH, USA [4]Division of Pathology, Cincinnati Children's Hospital Medical Center, Cincinnati, OH, USA [5]Virttu Biologics, Ltd, Glasgow, U.K. [6]Radboud University Medical Center, Radboud Institute for Molecular Life Sciences, Nijmegen The Netherlands [7]Department of Microbiology and Molecular Genetics, University of Pittsburgh, School of Medicine, Pittsburgh, PA, USA.

Abstract

Although most high-risk neuroblastomas are responsive to chemotherapy, relapse is common and long-term survival is less than 40%, underscoring the need for more effective treatments. We evaluated the responsiveness of 12 neuroblastoma cell lines to the $\Delta\gamma_1$34.5 attenuated oncolytic HSV, Seprehvir (HSV1716), which is currently used in pediatric phase I trials. We found that entry of Seprehvir in neuroblastoma cells is independent of the expression of nectin-1 and the sum of all four known major HSV entry receptors. We observed varying levels of sensitivity and permissivity to Seprehvir, suggesting that the cellular anti-viral response, not virus entry, is the key determinant of efficacy with this virus. *In vivo*, we found significant anti-tumor efficacy following Seprehvir treatment, which ranged from 6/10 complete responses in the CHP-134 model to a mild prolonged median survival in the SK-N-AS model. Taken together, these data suggest that anti-tumor efficacy cannot be solely predicted based on *in vitro* response. Whether or not this discordance holds true for other viruses or tumor types is unknown. Our results also suggest that profiling the expression of known viral entry receptors on neuroblastoma cells may not be entirely predictive of their susceptibility to Seprehvir therapy.

Correspondence: Pin-Yi Wang, Center for Childhood Cancer and Blood Disease, The Research Institute at Nationwide Children's Hospital, 700 Children's Drive, Columbus, OH 43205, USA. ; Email: pinyi.wang@nationwidechildrens.org, Phone: (614) 722-1394, Fax: (614) 722-3699

Conflict of Interest

JC is an employee of Virttu Biologics Ltd. The rest of the authors declare no conflict of interest.

Keywords

oHSV; neuroblastoma; HSV-1 entry receptor

Introduction

Neuroblastoma is the most common extra-cranial solid tumor of childhood. These tumors arise from the embryonic sympathoadrenal lineage of the neural crest and display extreme genetic and phenotypic heterogeneity. Neuroblastoma is a major cause of death for pediatric patients between ages one to five and is responsible for approximately 15% of childhood cancer-related deaths in the United States ([1]). Although most high-risk cases of neuroblastoma are responsive to chemotherapy and complete responses can be achieved, relapses are also fairly common and only 40% of patients survive long term. More effective treatments for this disease are clearly needed.

Oncolytic herpes virotherapy is an emerging form of therapy that utilizes attenuated herpes viruses to selectively infect and destroy cancerous tissue. Over the past decade, numerous preclinical models and clinical trials have demonstrated the efficacy and safety of this approach ([2, 3]), including a successful Phase III trial with the oncolytic herpes simplex virus (oHSV) Talimogene laherparepvec ([4]). Current oHSV vector designs mutate or selectively express the virulence factor $\gamma_1$34.5 as a means of restricting toxicity to tumor cells. Most oHSV vectors also retain their thymidine kinase gene (tk), making them susceptible to anti-herpetic agents in the unlikely event of an off-target infection ([5]).

HSV has a wide range of cellular tropism, partly due to its ability to interact with multiple entry receptors. These include the cellular adhesion molecules, nectin-1 and nectin-2 (for certain mutant strains), various moieties of heparin sulfate (HS), and TNF-receptor superfamily member 14, otherwise known as herpes virus entry mediator (HVEM) ([6]). The entry process begins when an enveloped virus attaches to heparin sulfate on the host cell surface via envelope glycoproteins B and C (gB and gC). This interaction allows the major receptor binding protein, glycoprotein D, to engage one of its receptors, triggering fusion of the viral envelope with the host cell membrane and the subsequent release of the virion into the cytosol. The virion can then traffic toward the cell nucleus, allowing transcription of the viral genome and the initiation of virus replication. Our laboratory and others have previously shown that HSV entry receptor expression on various cell types correlates with or determines their susceptibility to HSV infection ([7-10]). More recently, Jackson and colleagues reported that increasing nectin-1 expression in cell lines derived from malignant peripheral nerve sheath tumors enhanced the replication of wild-type HSV, but had no effect on the replication of $\Delta\gamma_1$34.5 viruses ([11]). Their study implies that cellular sensitivity to killing by such oHSV mutants is less dependent on the expression of virus entry receptors (susceptibility to infection) than it is on the host cell's ability to mount an anti-viral response (permissivity to infection).

Several studies have investigated the use of oHSV therapy in treating preclinical models of neuroblastoma and have shown significant anti-tumor efficacy with both $\gamma_1$34.5-intact and $\Delta\gamma_1$34.5 viruses ([12-14]). Whether the expression of viral entry receptors on neuroblastoma

cells contributes to the susceptibility (virus entry), sensitivity (virus-mediated cytotoxicity) and/or permissivity (productive virus infection) has not been thoroughly examined. In the present study, we evaluated the response of a panel of human neuroblastoma cell lines and preclinical neuroblastoma models to Seprehvir (a $\Delta\gamma_1$34.5 virus) treatment and examined the relationship between HSV entry receptor expression and anti-tumor efficacy. We show that human neuroblastoma cells express varying amounts of the known major HSV entry receptors with nectin-1 and 3-OS HS found in the greatest abundance. Conversely, levels of HVEM were virtually undetectable. The relative expression of any given HSV receptor by each cell line did not correlate with its sensitivity and susceptibility to Seprehvir *in vitro*. Our *in vivo* studies suggest that anti-tumor efficacy only partially correlates with virus production in the tumor. Furthermore, factors other than direct oncolysis, such as the induction of an innate immune cell response, may also contribute to the anti-tumor effect.

Results

oHSV Entry, Sensitivity and Susceptibility in Neuroblastoma Cells

We evaluated 12 human neuroblastoma cell lines for oHSV therapeutic potential in this study (see **Supplementary Figure S1** for demographic details). We first examined the ability of oHSV to enter each neuroblastoma cell line (classically defined as susceptibility). We infected each cell line with the clinical-grade oHSV Seprehvir (HSV1716) at a multiplicity of infection (MOI) of 20 infectious virus particles per cell. After 30 minutes of infection, the cells were washed with PBS and an acidic buffer solution to remove any bound, but non-internalized virus. We then isolated genomic DNA from each sample and determined the amount of HSV that had entered the cells via quantitative PCR (qPCR), normalizing copies of the HSV thymidine kinase gene (tk) to the house-keeping gene GAPDH. Our panel of neuroblastoma cell lines showed a wide range of susceptibility to Seprehvir infection, with the most susceptible lines (CHP-134 and CHLA-20) showing a five-fold increase in virus entry over the least susceptible cell lines (SH-SY5Y and NB-EBc1) (**Figure 1a**). These findings correlated well with virus entry studies using K26GFP, a wild-type KOS-strain oHSV that shares an identical gD protein (based on amino acid sequence) with Seprehvir **(Supplementary Figures S2 and S3)** ([15]).

Next, we evaluated the cytotoxicity and viral replication of Seprehvir within the 12 neuroblastoma cell lines. We quantified *in vitro* cytotoxicity with MTS cell survival assays conducted 6 days post virus infection (pvi). Representative cytotoxicity data from 4 of these cell lines (CHLA-20, CHP-134, SK-N-AS and SK-NBE2) are shown in **Figure 1b**, and illustrate a range of varying sensitivities to Seprehvir treatment. For comparative purposes, the IC_{50} values for the remaining neuroblastoma cell lines were graded and summarized in **Figure 1c**. To measure cell permissivity to virus, we evaluated Seprehvir replication in the same four cell lines at multiple timepoints following infection. In general, each cell line showed a steady increase in virus production over time, and the extent of this replication correlated well with each cell line's observed cytotoxicity; CHLA-20, the least sensitive of the neuroblastoma cell lines, showed only a <2 log increase in Seprehvir replication compared to the approximately 3.5 log increase seen in the more susceptible CHP-134 line (**Figure 1d**). Based on our observations, human neuroblastoma cells appear to respond

differently to Seprehvir treatment *in vitro*, with virus replication being more closely correlated to cytotoxicity than virus entry.

Evaluation of Herpes Simplex Virus-1 Entry Receptor Expression in Human Neuroblastoma Cell Lines

As HSV entry mainly relies on the binding of its surface glycoproteins to their cognate cellular receptors, we reasoned that it would be important to evaluate the expression of HSV-1 entry receptors in primary human neuroblastoma cases and further study their relationship with the overall response to oHSV therapy. To this end, we evaluated the expression of nectin-1 in a neuroblastoma tissue microarray (TMA) obtained from Children's Oncology Group (COG). This TMA contained primary neuroblastoma tumor specimens from 56 individual patients with different stages of disease. **Figure 2** shows representative nectin-1 immunohistochemical staining for several neuroblastoma variants, including both differentiated and undifferentiated forms of disease, a comparatively less aggressive ganglioneuroblastoma, and a benign ganglioneuroma. We assigned grades of nectin-1 expression for each specimen, ranging from negative to 3+. These data are summarized in **Table 1**. In total, 97% of the tested neuroblastoma specimens were found to express nectin-1 with the expression grade predominantly more than 2+, a finding consistent with previously reported data obtained from a smaller number of clinical specimens ([14]). Nectin-1 expression levels in these neuroblastoma specimens did not appear to be associated with the disease stage, NMYC status, age or sex (data not shown). We also profiled HSV entry receptor expression levels in our panel of neuroblastoma cell lines. The relative abundance of nectin-1, nectin-2, HVEM and 3-OS HS was determined by qRT-PCR (**Figure 3a**) and FACS analysis (**Figure 3b**). A heat map of these data, representing cell surface protein expression as quantified by mean fluorescence intensity values, is shown in **Figure 3c**. Each cell line expressed relatively high levels of 3-OS HS and moderate to high levels of nectin-1. Levels of nectin-2 and HVEM were considerably lower or absent altogether, suggesting that these receptors do not play significant roles in mediating HSV entry in neuroblastoma. In general, receptor RNA expression correlated well with surface protein expression, however we did observe some slight discordance with nectin-1 levels among the intermediate expressing cell lines. Likewise, the cell surface expression of nectin-2 by SK-N-SH, which we expected to be high based on qRT-PCR, was instead only moderate. Despite the high level of 3-OS HS in most neuroblastoma lines in the panel, we only detected relatively low levels of heparan sulfate 3-*O*-sulfotransferase 3 (HS3ST3), which previous studies used as an surrogate marker for 3-OS HS ([10], [16], [17]), indicating that other heparan sulfate 3-*O*-sulfotransferase isoforms ([18]) might be responsible for this receptor expression on neuroblastoma cells. We also mined the Pediatric Preclinical Testing Program (PPTP) gene expression database and found that most neuroblastoma xenograft tumors in that panel express relatively high levels of nectin-1 (**Supplementary Figure S4**, yellow columns, mRNA Z-score > 0) at the RNA level compared to other pediatric cancer models in the panel. Consistent with our findings, the PPTP database also showed lower than average expression of HVEM in neuroblastoma cells (**Supplementary Figure S4**, green columns, mRNA Z-score < 0). The mRNA levels of HS3ST3A1 and HS3ST3B1 were also low in this panel (**Supplementary Figure S4**, blue and purple columns). Given the fact that nectin-2 is selectively used by HSV-2 and only a subset of HSV-1 gD mutant strains ([19], [20]) as well as

the lack of HVEM expression in neuroblastoma cells, these data suggest that oHSV entry in neuroblastoma cells is mainly through nectin-1 and/or 3-OS HS. Nevertheless, the expression profile of nectin-1 or the sum of all four receptors did not correlate with virus entry or virus-mediated cytotoxicity as shown in **Figure 3d**. This discordance suggests that virus entry in neuroblastoma cells might involve additional unknown mediators and/or mechanisms.

Anti-Tumor Efficacy of oHSV in Xenograft Neuroblastoma Models

To determine the susceptibility of neuroblastoma tumors to oHSV therapy *in vivo*, four neuroblastoma lines were selected for survival studies based on their distinct HSV receptor profiles (shown in **Figure 3b**), MYCN status, and the duration of successful tumor engraftment in athymic nude mice (**Supplementary Figure S1**, highlighted). We treated mice with subcutaneously implanted tumors with intratumoral (ITu) injection of 1e7 plaque-forming units (pfu) of Seprehvir for a total of 3 doses at days 0, 2 and 4 when their tumor volumes reached 150-300 mm^3. Kaplan-Meier survival curves for the CHLA-20, CHP-134, SK-N-AS, and SK-N-BE(2) models are shown **Figure 4a-d**, respectively, with the corresponding tumor growth plots for each animal displayed in **Figure 4e-h**. Consistent with the *in vitro* killing assay, Seprehvir treated CHP-134 bearing mice showed the greatest anti-tumor efficacy (**Figure 4b**) with complete responses (CR) achieved in 6 out of 10 mice (**Figure 4f**). Seprehvir treatment in SK-N-AS tumors, the second most responsive line among the 12 *in vitro*, only slowed tumor growth, prolonging median survival from 14 days to 19 days (**Figure 4c and 4g**). Interestingly, tumors derived from CHLA-20, the least sensitive line *in vitro*, had a significant antitumor response to Seprehvir treatment, leading to complete responses in 3 out of 7 mice (**Figure 4a and 4e**). The remaining neuroblastoma model, SK-N-BE(2), initially showed some evidence of efficacy following Seprehvir treatment, but 6 out of 7 treated animals eventually succumbed to excessive tumor growth (**Figure 4d and 4h**).

Separate sets of tumor-bearing animals were used to assess *in vivo* Seprehvir replication. Unlike the animals in the previous efficacy studies, these mice received only a single 1e7 pfu dose of Seprehvir and were sacrificed at 3, 24, 72 and 144 hours thereafter. We then excised and processed their tumors to quantify virus production via HSV plaque assays (**Figure 5**). Similar to our *in vitro* observations (**Figure 1d**), Seprehvir replication was greatest in CHP-134 tumors, suggesting that the efficacy we observed in this model may be more dependent on direct oncolysis. Conversely, Seprehvir replication in the highly aggressive SK-N-AS model declined nearly 10-fold between 24 and 72 hours post infection, indicating that virus spread or replication in these tumors may be inadequate to slow tumor growth.

Because type I interferons are known to inhibit virus replication, we also sought to determine if differences in cellular responsiveness to exogenous type I interferons might explain differential virus production. We performed analyses of the interferon (IFN) response in these four cell lines by adding exogenous human IFN (mouse type I IFNs do not cross-react with human cells ([21])) and evaluating the induction of IFN-stimulated genes (ISGs). On this basis, we found that CHP-134 appears to be the least sensitive to IFN-beta treatment, which may partially explain why it is the most sensitive line both i*n vitro* and *in*

vivo (**Supplementary Figure S5**). However, our results do not adequately explain the disconnection between *in vitro* and *in vivo* efficacy observed in SK-N-AS, which displayed substantial induction of all 5 tested ISGs upon IFN-beta treatment. Therefore, we think the IFN response may only partially explain the differences of how cells react to virus treatment in our study, and other factors, such as infiltrating immune cells and the concomitant cytokine response may also play a role.

Discussion

The cure of high-risk neuroblastoma patients remains an ongoing challenge. Despite significant advancements in our understanding of this disease and its management, overall survival rates remain unacceptably low and provide an impetus to develop novel and more effective therapies. Attenuated oncolytic herpes viruses such as Seprehvir are promising therapeutic agents not only because they can safely and selectively destroy cancerous cells and release progeny virus to do likewise (the central paradigm of oncolytic virotherapy), but also because of their ability to stimulate an anti-tumor immune response. Two ongoing clinical trials are investigating the use of Seprehvir in young patients with either CNS (NCT02031965) or non-CNS (NCT00931931) solid tumors, the latter including patients with neuroblastoma.

In this study we evaluated a panel of 12 human neuroblastoma cell lines for their expression of HSV entry mediators and assessed their responses to Seprehvir treatment. Most cells showed high expression of nectin-1 and 3-OS HS, two HSV entry receptors that have been shown to be important determinants of HSV susceptibility in various cell types ([8], [9], [16], [17]) Unexpectedly, we found that HSV receptor expression did not necessarily correlate with virus entry. For example, the neuroblastoma cell line NB-1643, which had the highest overall expression of nectin-1 in addition to high levels of 3-OS HS, fell into the relatively low virus uptake group (**Figures 1a** and **3c**). Likewise, IMR-32, one of the highest 3-OS HS expressing cells, also showed lower virus uptake (**Figure 1a** & **3c**). Although the PCR-based assay we used for virus entry study only measures an average value over the entire population of cells, we consistently observe a Poisson distribution of gene expression when using flow cytometry and GFP-expressing oHSVs (not shown). Thus, some cells are more susceptible than others and our assay doesn't allow us to correlate virus entry with permissivity on a cell-by-cell basis. Nevertheless, our finding of a discordance of receptor expression with entry in cells on average could indicate that i) other unknown entry receptors may be expressed and utilized in neuroblastoma cells or, ii) nectin-1 or other receptor-mediated viral entry pathways do not function properly in some of these neuroblastoma lines ([22]). Interestingly, although we did not see a correlation between Seprehvir entry and cytotoxicity, we did find a correlation between entry of the wild-type ($\gamma_1$34.5-intact) K26GFP virus and viral gene transfer (GFP) (**Supplementary Figures S2 and S3b**). This finding suggests that something other than susceptibility (entry) is responsible for sensitivity to Seprehvir killing, such as cell-autonomous anti-viral responses, which would be in agreement with a recent report from Jackson and colleagues ([11]). Whatever the case, profiling neuroblastoma tumor cells for currently known HSV entry receptors does not appear be predictive for determining the degree of their susceptibility to oHSV.

We observed similar variability *in vivo*, where peak levels of Seprehvir replication in SK-N-AS tumors were comparable to those achieved in the better responding CHLA-20 and SK-N-BE(2) tumor models. We postulate that the failure of Seprehvir to induce a complete response in the SK-N-AS model may be due to the high intrinsic growth rate of these tumors relative to our other models (**Figure 4**, PBS-treated tumors), and that tumor cell proliferation may simply outpace virus replication in that model. Conversely, the relative resistance of CHLA-20 to Seprehvir *in vitro* may mainly due to its autonomous anti-viral responses as its *in vitro* growth rate is similar to SK-NBE(2) and relative slower than CHP-134 (**Supplementary Figure S6**).

Another possibility is that discrete differences amongst the tumor microenvironments of the neuroblastoma models may be influencing the therapeutic response. Preliminary cell recruitment studies performed in these four neuroblastoma models show that Seprehvir treatment induces the infiltration of differential leukocyte subsets, including many key components of the innate immune response (unpublished data). Further studies will need to be conducted to understand the contribution of each of these components in the antitumor activity of Seprehvir in neuroblastoma, but are beyond the scope of this present work.

In support of this concept, it is well established that wild-type HSV infection induces both innate and adaptive immune responses within the host, including the recruitment of immune effector cells and the production of inflammatory cytokines ([23]). Our lab and others have demonstrated that this response also occurs within the context of oncolytic herpes virotherapy ([21, 24–27]). We previously showed that oHSV treatment of the A673 Ewing sarcoma model led to a concomitant influx of $CD11b^+$ myeloid cells (monocytes/macrophages, granulocytes, natural killer cells, etc.) into the tumor. The net effect of this cellular infiltration was a dampening of oHSV therapeutic efficacy, as tumor growth was further delayed when these $CD11b^+$ cell populations were depleted ([26]). More recently, we demonstrated that tumor shrinkage in syngeneic rhabdomyosarcoma models following oHSV treatment was not mediated by direct oncolysis, but rather by the induction of anti-tumor T-cells ([21]). Similar studies by Workenhe et al. suggest that the immunogenic cell death caused by HSV can lead to further activation of anti-tumor immunity (mainly via CD8+ T cells), which may be more important to a positive treatment outcome than the persistence of virus replication ([28]). The relative roles of virolysis versus immunologic response in tumor shrinkage has been a major issue for discussion in the field, which continues to pose a conundrum for preclinical testing; while human tumors are typically the most susceptible to human virus infection, animals bearing human tumor xenografts lack an adaptive immune response. Conversely, mouse tumors in immunocompetient animals are typically not very susceptible and/or permissive to human viruses. Certainly this difference exists for human herpes simplex viruses. Thus studies in human xenografts typically only measure lytic or innate immunologic effects, whereas studies in mouse tumors primarily measure immunologic effects. To complicate matters further, there are species-specificities with respect to molecular interactions, particularly for the immune system. In light of these observations, we are presently conducting studies to better understand how the tumor microenvironment affects oHSV therapy in both xenograft and syngenic in various pediatric tumor models.

In summary, our study demonstrates that Seprehvir is differentially effective amongst neuroblastoma cell lines and *in vitro* cytotoxicity is not completely predictive of *in vivo* therapeutic response. *In vitro* sensitivity appears to be less related to the host cell's expression of putative HSV entry receptors than it is to permissiveness of virus replication. While virus replication appears to be important for the *in vivo* neuroblastoma therapeutic response, it is also not the sole determinant of efficacy, and other factors such as the tumor microenvironment are likely modulating the anti-tumor response.

Material and Methods

Cells and viruses

All neuroblastoma cell lines in the study were either directly purchased from ATCC or requested from the Pediatric Preclinical Testing Program (PPTP, http://gccri.uthscsa.edu/pptp/). In addition, the identities of all cell lines used in the study were confirmed by Short Tandem Repeats verification and tested free of mycoplasma using MycoAlert™ Mycoplasma Detection Kit (LT07-318, Lonza Inc. Allendale, NJ). CHLA-20, CHLA-90, CHLA-119 and CHLA-136 were cultured in IMDM containing 20% FBS, 1% Insulin-Transferrin-Selenium (ITS -G) (41400-045, Thermo Fisher Scientific Inc. Waltham, MA) and penicillin/streptomycin (100 U/mL and 100 μg/mL, respectively). CHP-134, IMR-32 and SK-N-SH were cultured in EMEM with 10% FBS and penicillin/streptomycin. NB-1643, NB-EBc1 and SK-N-AS were cultured in DMEM with 10% FBS and penicillin/streptomycin. SK-N-BE(2) and SH-SY5Y were culture in EMEM/F-12 (1:1) with 10% FBS and penicillin/streptomycin. Vero cells (ATCC, Manassas, VA), were cultured in EMEM with 10% FBS and penicillin/streptomycin. The wild-type gD virus (K26GFP) has been described previously([15]) and oncolytic HSV, Seprehvir (HSV1716)([29]) was a gift from Virttu Biologics Ltd. (Glasgow, U.K.)

Viral entry assay

5×10^5 cells were placed in a tube in the culture medium and infected with HSV at MOI of 20 in triplicate and remained on ice for 30mins for virus attachment with gentle mixing every 10mins. The cultures were then shifted into 37°C. After 30mins incubation, cells were spun down and washed with acid-glycine buffer for 2 sec followed by PBS wash. Cell pellets were collected and genomic DNA (gDNA) was isolated via QIAamp DNA Mini Kit (Qiagen, Valencia, CA). The sample gDNA was used as the template for quantitative PCR (qPCR, see below) to quantify viral genomes in the cells, 5ng per reaction in triplicates (n=3). Known quantities of GAPDH and HSV-tk PCR fragments were used to generate standard curves for qPCR analysis. Data are presented as the HSV-tk DNA copies per GAPDH. Primer sequence for GAPDH, amplicon size 274bp, forward: ACATCATCCCTGCCTCTAC, reverse: CCACTCCTCCACCTTTGA; for HSV-tk, amplicon size 154bp, forward: TCC GCC TGG AGC AGA AAA TG, reverse: AAC ACC CGC CAG TAA GTC ATC. Results shown are the mean of two independent experiments. Error bars represent s.e.m (n=6).

RNA extraction, Reverse transcription PCR and Quantitative PCR

Total RNA was isolated from 1×10^6 cells using the RNeasy Plus Mini Kit (Qiagen) per manufacturer's instructions. The concentration and purity of the recovered RNA was determined measuring the optical density at 260 and 280 nm. cDNA was generated using SuperScript™II Reverse Transcriptase (Thermo Fisher Scientific Inc.) per the manufacturer's instructions. For qPCR, 5 μL of *Power* SYBR® Green PCR Master Mix (Thermo Fisher Scientific Inc.), 5 μL of 1:25 diluted cDNA and 500 nM of each primer of interest was used in a 10 μL reaction. The reaction was performed using a 7900 Real-Time PCR System (Thermo Fisher Scientific Inc.). The samples were run at 50°C for 2 minutes, 95°C for 10 minutes, 40 cycles of 94°C for 15 seconds, 58°C for 35 seconds, and 72°C for 35 seconds followed by a standard dissociation stage to determine the melting temperature of each amplification product. The comparative quantitation method was used for data analysis. The results were presented as expression fold relative to GAPDH : $2^{-(C_t \text{ target gene-}C_t GAPDH)}$. Primers used in the study were described previously ([10]). Results shown are representative of three independent experiments.

Flow cytometry

Single-cell suspensions of approximately $1{\times}10^6$ elements were treated with 10% FcR blocking reagent (130-059-901, Miltenyi Biotec Inc. Auburn, CA) for 10 min at 4°C and then stained with anti-human nectin-1 (R1.302.12) (sc-69718, Santa Cruz Biotechnology, Inc. Dallas, TX), nectin-2 (R2.525) (sc-32804, Santa Cruz Biotechnology, Inc.) or HVEM (CW10) (sc-21718, Santa Cruz Biotechnology, Inc.). After applying the unconjugated primary Abs or their isotype controls, cells were stained with a secondary FITC-conjugated goat anti-mouse IgG (554001, BD Biosciences, San Jose, CA). For 3-O-Sulfated Heparan Sulfate (3-OS HS) analysis, cells were first fixed in 1% paraformaldehyde (PFA) for 10 min at 4°C followed by incubation with antibody HS4C3 ([30]) for 1 hour at 4°C. Next, cells were stained with unconjugated mouse anti-VSV (P5D4) (V5507, Sigma-Aldrich Corp. St. Louis, MO) for 30 min at 4°C. Finally, cells were stained with FITC goat anti-mouse Ig (554001, BD Biosciences) for 20 mins at 4°C. The analysis has been performed on the neuroblastoma panel for three independent times. Average mean fluorescence intensities (MFI) of nectin-1, nectin-2, HVEM and 3-OS HS relative to isotype (for netin-1, nectin-2 and HVEM) or unstained controls (for 3-OS HS) were calculated and presented as a heatmap in Figure 3c.

Tissue microarray and immunohistochemistry

Neuroblastoma tissue microarray chips were obtained from Children's Oncology Group (Nationwide Children's Hospital, Columbus OH) that contained neuroblastoma specimens from 56 individual patients. For immunohistochemistry staining, the reagents described below were all from Ventana Medical Systems, Inc. Tucson, Arizona. After deparaffinization, slides were pre-treated with Cell Conditioning 1 (CC1, #950-124) for 90 minutes for antigen retrieval, incubated with the nectin-1 antibody (R1.302.12, Santa Cruz Biotech) at 1:10 dilution for 2 hours at 42 °C, followed by blocking the slides for 8 minutes with blocking reagent (#760-1028), stained with hematoxylin (#760-2021) for 4 minutes, and Bluing Reagent (#760-2037) for 4 minutes. The slides were then subjected for detection using UltraView detection kit (#760-500) per manufacture's protocol. The degree of nectin-1

staining intensity of tumor samples was graded negative as 0, weak as 1+, moderate as 2+, and strong as 3+, by board-certified pathologist, M.H.C

Cell survival/MTS assay

Cells were plated in 96-well dishes at 4000 cells/well, incubated at 37°C for overnight and then infected with Seprehvir at MOI 0.001, 0.01, 0.1 and 1.0 in hexaplicate. The assays were performed using Cell Titer96 AQueous Non-Radioactive Cell Proliferation Assay (G5421, Promega, Madison, WI) per manufacturer's instructions on days 2, 4 and 6. Results were presented as percent cell survival compared to uninfected controls. Results shown are representative of three independent experiments.

In vitro virus production

Neuroblastoma cell lines were plated in 12-well dishes at 5×10^4 cells per well in triplicate, incubate at 37°C overnight, and infected with Seprehvir at MOI 0.01. Plates were gently shaken every 20 minutes for 2 hours. At 2, 24, 48 and 72 hours post infection, both cells and supernatants were harvested, freeze-thawed three times, diluted, and titered by standard plaque assay on Vero cells.

Animal studies

Animal studies were approved by the Nationwide Children's Hospital Institutional Animal Care and Use Committee (IACUC), protocol number AR12-00045. To establish tumors, 5×10^6 of CHLA-20, CHP-134, SK-N-AS and SK-N-BE(2) cells were injected subcutaneously with 33% Matrigel (356234, BD Biosciences) into the flanks of 5-6 week-old female athymic nude mice (Harlan Laboratories, Inc. Indianapolis, IN). When tumors reached 150-300 mm^3, animals were pooled and randomly assigned into 2 groups. One group of mice was treated intratumorally (ITu) with Seprehvir (10^7 pfu in 100 μL) every other day for a total of 3 injections. Control mice received ITu PBS following the same regimen. Tumor volume was determined by $V = (L \times W^2)\pi/6$, where L is the length of the tumor and W is the width. Animals were monitored for tumor volumes two times per week not blinded for 80 days after initial treatment, until tumor volume exceeded 2500mm^3, or until tumor diameter reached 2 cm. Initial sample size was estimated based on previous study([31]) for 10 mice per group. Animals that did not have successful tumor engraftment within the estimated period (see Supplementary Figure S1 for the time length of tumor growth) were excluded from the study.

In vivo virus production

Subcutaneous xenografted human neuroblastoma tumors were established in 5-6 week-old athymic nude mice as described above. Tumors were treated with one dose of Seprehvir (10^7 pfu in 100 μL) intratumorally when reached 350-500 mm^3. Tumors were then harvested at 3, 24, 72 and 144 hours pvi, four tumors per time point, followed by homogenizing, freeze-thawed three times and the lysates were titered by standard plaque assay (triplicates) on Vero cells.

Statistical Analysis

All statistical analyses were performed using Statistical Analysis System software 9.3 (SAS Institute., Cary, NC, USA). Statistics for figure 1b and 1d were analyzed using linear mixed models adjusted for unequal variances to compare cell groups. For figure 1b, survival for the four cell groups was compared over different MOIs. For figure 1d, viral titer (measured as log PFU) was compared over time for each of the four cell groups. Figures 1b and 1d have 95% confidence limits to aid in showing where statistically significant differences exist between the cell groups. For figure 4a-d Kaplan-Meier survival curves were analyzed by log-rank test to compare the survival of Seprehvir and PBS. In figure 5, Bonferroni corrected pairwise comparisons were made to look for differences in virus yields (PFU) amongst the four groups at 24 hours (** for p-value < .01).

Supplementary Material

Refer to Web version on PubMed Central for supplementary material.

Acknowledgement

We thank Brian Geier for analysis of the Pediatric Preclinical Testing Program gene expression database, and Peter Houghton (Greehey Children's Cancer Research Institute) for cell lines. This work was supported in part by Alex's Lemonade Stand Foundation for Childhood Cancer (PYW), the Research Institute at Nationwide Children's Hospital, and NIH grant R21-CA133663-01A1 (TPC).

Oncolytic HSV Seprehvir used in the study was from Virttu Biologics, Ltd (Glasgow, UK).

References

1. Park JR, Eggert A, Caron H. Neuroblastoma: biology, prognosis, and treatment. Pediatric clinics of North America. 2008; 55(1):97–120, x. [PubMed: 18242317]
2. Patel MR, Kratzke RA. Oncolytic virus therapy for cancer: the first wave of translational clinical trials. Transl Res. 2013; 161(4):355–64. [PubMed: 23313629]
3. Pol J, Bloy N, Obrist F, Eggermont A, Galon J, Cremer I, et al. Trial Watch:: Oncolytic viruses for cancer therapy. Oncoimmunology. 2014; 3:e28694. [PubMed: 25097804]
4. Andtbacka RH, Kaufman HL, Collichio F, Amatruda T, Senzer N, Chesney J, et al. Talimogene Laherparepvec Improves Durable Response Rate in Patients With Advanced Melanoma. Journal of clinical oncology : official journal of the American Society of Clinical Oncology. 2015
5. Balfour HH Jr. Antiviral drugs. N Engl J Med. 1999; 340(16):1255–68. [PubMed: 10210711]
6. Spear PG. Herpes simplex virus: receptors and ligands for cell entry. Cell Microbiol. 2004; 6(5): 401–10. [PubMed: 15056211]
7. Huang YY, Yu Z, Lin SF, Li S, Fong Y, Wong RJ. Nectin-1 is a marker of thyroid cancer sensitivity to herpes oncolytic therapy. J Clin Endocrinol Metab. 2007; 92(5):1965–70. [PubMed: 17327376]
8. Yu Z, Adusumilli PS, Eisenberg DP, Darr E, Ghossein RA, Li S, et al. Nectin-1 expression by squamous cell carcinoma is a predictor of herpes oncolytic sensitivity. Molecular therapy : the journal of the American Society of Gene Therapy. 2007; 15(1):103–13. [PubMed: 17164781]
9. Friedman GK, Langford CP, Coleman JM, Cassady KA, Parker JN, Markert JM, et al. Engineered herpes simplex viruses efficiently infect and kill CD133+ human glioma xenograft cells that express CD111. Journal of neuro-oncology. 2009; 95(2):199–209. [PubMed: 19521665]
10. Wang PY, Currier MA, Hansford L, Kaplan D, Chiocca EA, Uchida H, et al. Expression of HSV-1 receptors in EBV-associated lymphoproliferative disease determines susceptibility to oncolytic HSV. Gene Ther. 2013; 20(7):761–9. [PubMed: 23254370]

11. Jackson JD, McMorris AM, Roth JC, Coleman JM, Whitley RJ, Gillespie GY, et al. Assessment of oncolytic HSV efficacy following increased entry-receptor expression in malignant peripheral nerve sheath tumor cell lines. Gene Ther. 2014; 21(11):984–90. [PubMed: 25119379]
12. Parikh N, Currier MA, Adams LC, Mahller YY, DiPasquale B, Collins MH, et al. Oncolytic herpes simplex virus mutants are more efficacious than wild-type adenovirus for the treatment of high-risk neuroblastomas in preclinical models. Pediatric Blood Cancer. 2005; 44:469–78. [PubMed: 15570577]
13. Mahller YY, Williams JP, Baird WH, Mitton B, Grossheim J, Saeki Y, et al. Neuroblastoma cell lines contain pluripotent tumor initiating cells that are susceptible to a targeted oncolytic virus. PLoS ONE. 2009; 4(1):e4235. [PubMed: 19156211]
14. Gillory LA, Megison ML, Stewart JE, Mroczek-Musulman E, Nabers HC, Waters AM, et al. Preclinical evaluation of engineered oncolytic herpes simplex virus for the treatment of neuroblastoma. PLoS One. 2013; 8(10):e77753. [PubMed: 24130898]
15. Desai P, Person S. Incorporation of the green fluorescent protein into the herpes simplex virus type 1 capsid. Journal of virology. 1998; 72(9):7563–8. [PubMed: 9696854]
16. Tiwari V, Clement C, Xu D, Valyi-Nagy T, Yue BY, Liu J, et al. Role for 3-O-sulfated heparan sulfate as the receptor for herpes simplex virus type 1 entry into primary human corneal fibroblasts. Journal of virology. 2006; 80(18):8970–80. [PubMed: 16940509]
17. Choudhary S, Marquez M, Alencastro F, Spors F, Zhao Y, Tiwari V. Herpes simplex virus type-1 (HSV-1) entry into human mesenchymal stem cells is heavily dependent on heparan sulfate. J Biomed Biotechnol. 2011; 2011:264350. [PubMed: 21799659]
18. Tiwari V, Tarbutton MS, Shukla D. Diversity of heparan sulfate and HSV entry: basic understanding and treatment strategies. Molecules. 2015; 20(2):2707–27. [PubMed: 25665065]
19. Warner MS, Geraghty RJ, Martinez WM, Montgomery RI, Whitbeck JC, Xu R, et al. A cell surface protein with herpesvirus entry activity (HveB) confers susceptibility to infection by mutants of herpes simplex virus type 1, herpes simplex virus type 2, and pseudorabies virus. Virology. 1998; 246(1):179–89. [PubMed: 9657005]
20. Lopez M, Cocchi F, Menotti L, Avitabile E, Dubreuil P, Campadelli-Fiume G. Nectin2alpha (PRR2alpha or HveB) and nectin2delta are low-efficiency mediators for entry of herpes simplex virus mutants carrying the Leu25Pro substitution in glycoprotein D. Journal of virology. 2000; 74(3):1267–74. [PubMed: 10627537]
21. Leddon C-YC, Jennifer L.; Currier, Mark A.; Wang, Pin-Yi; Jung, Francesca A.; Denton, Nicholas L.; Cripe, Kevin M.; Haworth, Kellie B.; Arnold, Michael A.; Gross, Amy C.; Eubank, Timothy D.; Goins, William F.; Glorioso, Joseph C.; Cohen, Justus B.; Grandi, Paola; Hildemanand, David A.; Cripe, Timothy P. Oncolytic HSV virotherapy in murine sarcomas differentially triggers an antitumor T-cell response in the absence of virus permissivity. Molecular Therapy — Oncolytics. 2015; 1:14010. [PubMed: 27119100]
22. Uchida H, Shah WA, Ozuer A, Frampton AR Jr. Goins WF, Grandi P, et al. Generation of herpesvirus entry mediator (HVEM)-restricted herpes simplex virus type 1 mutant viruses: resistance of HVEM-expressing cells and identification of mutations that rescue nectin-1 recognition. Journal of virology. 2009; 83(7):2951–61. [PubMed: 19129446]
23. Chew T, Taylor KE, Mossman KL. Innate and adaptive immune responses to herpes simplex virus. Viruses. 2009; 1(3):979–1002. [PubMed: 21994578]
24. Miller CG, Fraser NW. Role of the immune response during neuro-attenuated herpes simplex virus-mediated tumor destruction in a murine intracranial melanoma model. Cancer Res. 2000; 60(20):5714–22. [PubMed: 11059765]
25. Alvarez-Breckenridge CA, Yu J, Price R, Wojton J, Pradarelli J, Mao H, et al. NK cells impede glioblastoma virotherapy through NKp30 and NKp46 natural cytotoxicity receptors. Nat Med. 2012; 18(12):1827–34. [PubMed: 23178246]
26. Currier MA, Eshun FK, Sholl A, Chernoguz A, Crawford K, Divanovic S, et al. VEGF blockade enables oncolytic cancer virotherapy in part by modulating intratumoral myeloid cells. Molecular therapy : the journal of the American Society of Gene Therapy. 2013; 21(5):1014–23. [PubMed: 23481323]

27. Thorne AH, Meisen WH, Russell L, Yoo JY, Bolyard CM, Lathia JD, et al. Role of cysteine-rich 61 protein (CCN1) in macrophage-mediated oncolytic herpes simplex virus clearance. Molecular therapy : the journal of the American Society of Gene Therapy. 2014; 22(9):1678–87. [PubMed: 24895995]

28. Workenhe ST, Simmons G, Pol JG, Lichty BD, Halford WP, Mossman KL. Immunogenic HSV-mediated oncolysis shapes the antitumor immune response and contributes to therapeutic efficacy. Molecular therapy : the journal of the American Society of Gene Therapy. 2014; 22(1):123–31. [PubMed: 24343053]

29. MacLean AR, ul-Fareed M, Robertson L, Harland J, Brown SM. Herpes simplex virus type 1 deletion variants 1714 and 1716 pinpoint neurovirulence-related sequences in Glasgow strain 17+ between immediate early gene 1 and the 'a' sequence. J Gen Virol. 1991; 72(Pt 3):631–9. [PubMed: 1848598]

30. Ten Dam GB, Kurup S, van de Westerlo EM, Versteeg EM, Lindahl U, Spillmann D, et al. 3-O-sulfated oligosaccharide structures are recognized by anti-heparan sulfate antibody HS4C3. J Biol Chem. 2006; 281(8):4654–62. [PubMed: 16373349]

31. Currier MA, Eshun FK, Sholl A, Chernoguz A, Crawford K, Divanovic S, et al. VEGF blockade enables oncolytic cancer virotherapy in part by modulating intratumoral myeloid cells. Molecular Therapy. 2013; 21(5):1014–23. [PubMed: 23481323]

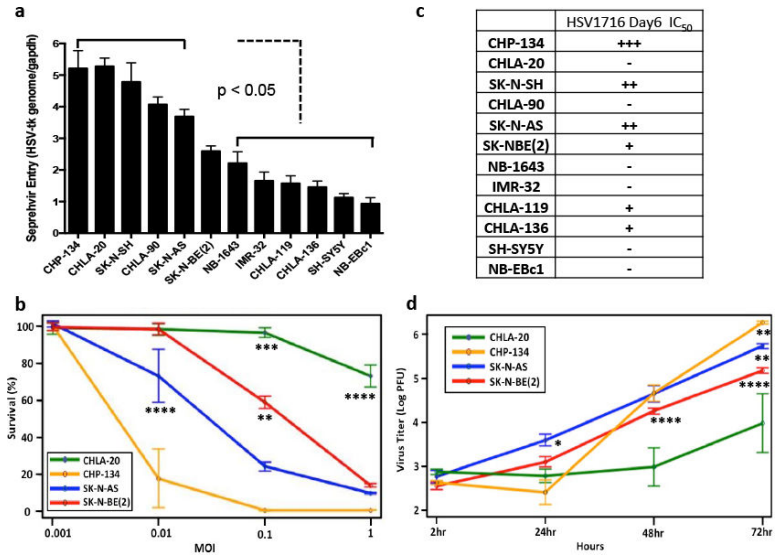

Figure 1. Neuroblastoma cell lines display differential responses to oHSV treatment *in vitro*

(a) *In vitro* virus entry assay. Cells were infected with Seprehvir (MOI=20) for 30 mins prior to genomic DNA isolation and qPCR analysis. Data are presented as HSV-*tk* gene copies per *Gapdh*. Error bars represent s.e.m. (n=6). (b) *In vitro* cytotoxicity of oHSV in neuroblastoma cells. Cells were infected with Seprehvir at MOIs of 0.001, 0.01, 0.1 and 1.0 and MTS viability assays were performed 6 days post virus infection. Cell survival is presented as the percent of viable cells compared to uninfected controls. Data are presented as a mean plot to compare cell survival among MOI and cell group with 95% confidence limits (standard error, n=6). (c) Day6 IC_{50} of Seprehvir for the 12 neuroblastoma cell lines. +++ indicates IC_{50} falls between MOI 0.001-0.01; ++ means IC_{50} falls between MOI 0.01-0.1; + indicates IC_{50} falls between MOI 0.1-1; − represents IC_{50} > MOI=1.(d) *In vitro* virus replication assay. Neuroblastoma cells were treated with Seprehvir at MOI=0.01 and virus yields were determined by plaque assays performed 2, 24, 48 and 72 hours post virus infection. Data are presented as a mean plot for virus titer over time with 95% confidence limit (standard error, n=9). Linear Mixed Model with Tukey-adjusted p-values is used for multiple comparisons. *p<0.05, ** p<0.01, *** p<0.001 and **** p<0.0001.

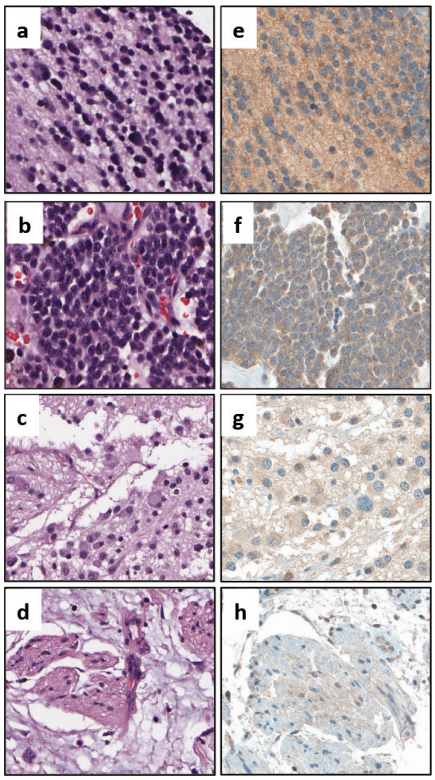

Figure 2. Nectin-1 expression by different primary neuroblastoma specimens

Representative H&E and nectin-1 immunohistochemical staining for (a,e) differentiated neuroblastoma, (b,f) undifferentiated neuroblastoma, (c,g) ganglioneuroblastoma, and (d,h) ganglioneuroma.

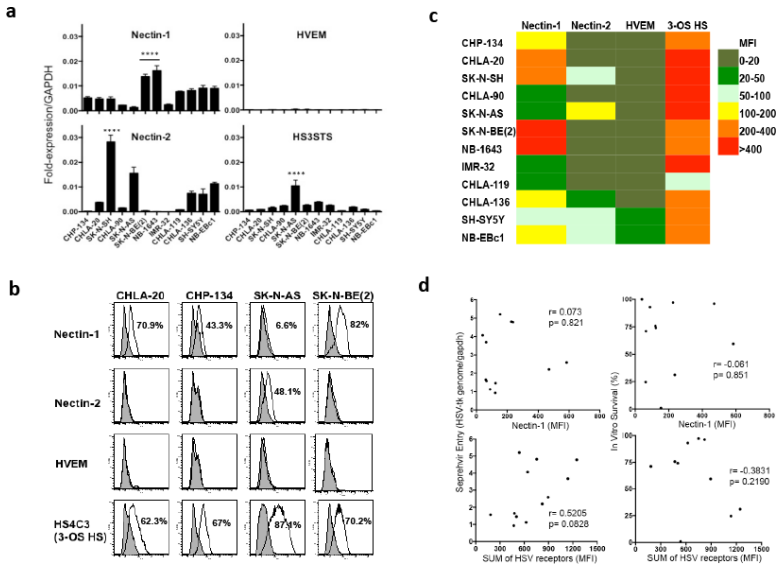

Figure 3. HSV entry receptor expression in the neuroblastoma cell line panel

(a) Quantitative RT-PCR analysis for mRNA expression of nectin-1, nectin-2, herpes virus entry mediator (HVEM) and heparin sulfate (glucosamine) 3-O-sulfotransferase 3 (HS3ST3, surrogate marker for 3-OS HS). Data are presented relative to *Gapdh*. Error bars represent s.d. (n=3). Linear Mixed Model with Tukey-adjusted p-values is used for multiple comparisons. The expression levels of Nectin-1, Nectin-2 or HS3STS in the indicated cell lines are significant higher than the rest. **** $p<0.0001$. (b) Representative FACS analysis of the HSV entry receptors in four select neuroblastoma cell lines. (c) A heat map summarizing the surface HSV-1 receptor expression profile of the 12 neuroblastoma cell lines. Data are presented as average mean fluorescence intensities (MFI) of nectin-1, nectin-2, HVEM and 3-OS HS relative to isotype or unstained controls from three independent results as determined by FACS. (d) Correlation of nectin-1 or the sum of HSV entry receptors expression with Seprehvir entry and cytotoxicity in neuroblastoma cell panel. Pearson's correlation coefficients were calculated between nectin-1/the sum of all four HSV entry receptors expression and virus entry (Figure 1a) or cell survival following Seprehvir treatment (Figure 1c).

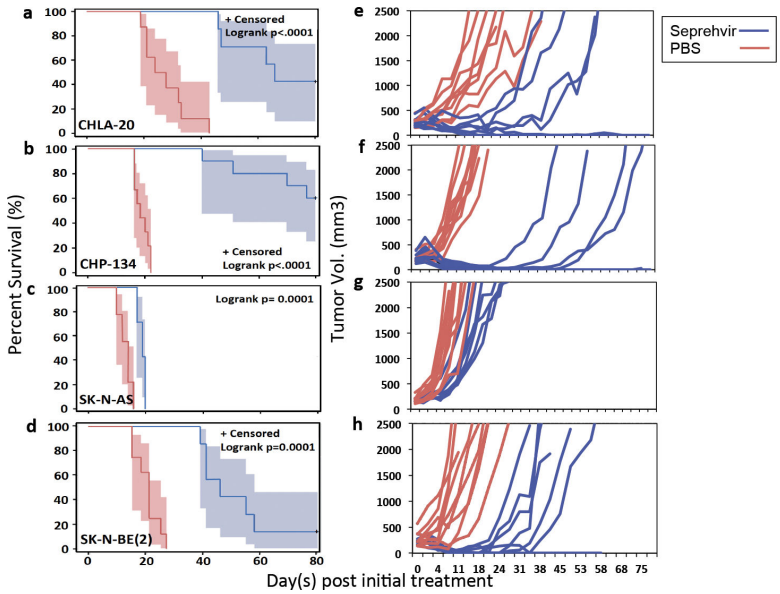

Figure 4. Intratumoral Seprehvir treatment significantly prolongs survival and delays or reverses tumor progression in neuroblastoma xenograft models

Mice bearing subcutaneous neuroblastoma tumors received intratumoral injections of PBS (red line), or 10^7 pfu Seprehvir (blue line) for a total of 3 treatments at days 0, 2 & 4 after the tumor mass reached 150–300mm^3. Tumors were measured twice a week after virus infection. Mice were sacrificed when the tumor size reached 2500mm^3 or due to the appearance of morbidity. Kaplan–Meier survival curves with 95% confidence limits were plotted and scored for statistical significance with the log-rank test for the results of (a) CHLA-20, n=8 (PBS), n=7 (Seprehvir), (b) CHP-134, n=9 (PBS), n=10 (Seprehvir), (c) SK-N-AS, n=9 (PBS), n=7 (Seprehvir) and (d) SK-N-BE(2), n=8 (PBS), n=7 (Seprehvir), tumor models. Panels (e-h) show corresponding tumor growth curves for the individual mice in each treatment group.

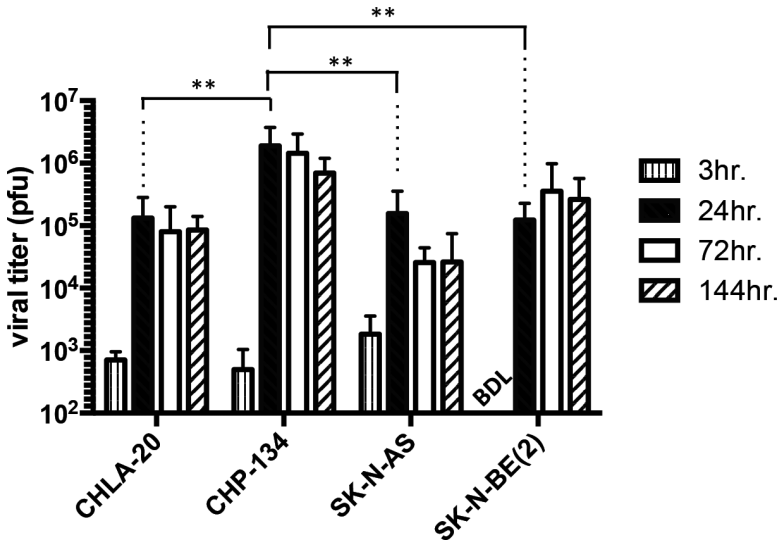

Figure 5. Seprehvir replication in neuroblastoma xenograft tumors

Subcutaneously implanted CHLA-20, CHP-134, SK-N-AS and SK-NBE(2) tumors were given a single ITu dose of 10^7pfu Seprehvir and harvested at 3, 24, 72 and 144 hours post infection for plaque assay. Data are presented as mean plaque forming unit (pfu) per tumor from triplicate plaque assays of four tumors at each time point. Error bars represent s.d. (n=12). Bonferroni corrected pairwise comparisons were made to look for differences in virus yields (PFU) amongst the four groups at 24 hours. ** $p<0.01$. BDL, below detectable level.

Table. 1

Summary of Nectin-1 expression level on neuroblastoma tissue microarray

Clinical Information			Number of Cases			
Histology	**Stage**	**Cell type**	**0**	**1+**	**2+**	**3+**
Neuroblastoma	I	Neuroblast			5	4
		Neuropil			4	3
	II	Neuroblast	1		4	5
		Neuropil	1		1	5
	III	Neuroblast			2	5
		Neuropil			2	4
	IV	Neuroblast	1	3	6	16
		Neuropil	1	4	6	15
Ganglioneuroma	N/A	Ganglion			2	
Ganglioneuroblastoma		Neuroblast				3
		Neuropil		2		
Tonsil	N/A	N/A				3
	Total NB cases		2	4	17	33
	Percentage		**3%**	**7%**	**30%**	**59%**

56 primary neuroblastoma samples were subjected to IHC staining to detect nectin-1 expression. The degree of nectin-1 staining intensity of tumor samples was graded negative as 0, weak as 1+, moderate as 2+, and strong as 3+, by board-certified pathologist, M.H.C